

# ANALYSIS OF PROTECTED RIA AND LOFA IN PLATE TYPE RESEARCH REACTOR USING COUPLED NEUTRONICS THERMAL-HYDRAULICS SYSTEM CODE

**Marat Margulis and Erez Gilad\***

The Unit of Nuclear Engineering  
Ben-Gurion University of the Negev, Beer-Sheva 84105, Israel  
[maratm@post.bgu.ac.il](mailto:maratm@post.bgu.ac.il); [gilade@bgu.ac.il](mailto:gilade@bgu.ac.il)

## ABSTRACT

The application of Best Estimate (coupled neutron kinetics/thermal-hydraulics - NK/TH) codes for research reactors safety analyses has gained considerable momentum during the past decade. This activity is largely facilitated by the high level of technological maturity and expertise attained by these techniques as NPPs safety technology and is largely driven by IAEA activities. The present study belongs in this framework, where a coupled NK/TH code (THERMO-T) was developed and applied to the analysis of protected reactivity insertion (RIA) and loss of flow (LOFA) accidents in a typical research reactor with standard MTR plate type fuel assemblies. The coupling is realized by considering the neutronic reactivity feedbacks of the fuel and coolant temperatures and a heat generation model for the reactor power. The neutron flux in the reactor core is solved by applying the point reactor kinetic equations, using radial and axial power distributions calculated from a 3D full core model by the three-dimensional continuous-energy Monte Carlo reactor physics code Serpent. The evolution of temporal and spatial distributions of both fuel and coolant temperatures is calculated for all fuel channels using a finite volumes time implicit numerical scheme for solving a three conservation equations model. In this study, three different thermal hydraulic models of the code are evaluated, as well as its sensitivity to different heat transfer correlations.

## KEYWORDS

Research reactor, transients, safety analysis, LOFA, RIA, coupled system code

## 1. INTRODUCTION

Research Reactors (RRs) are developed and built primarily as test facilities and neutron generators for vast range of scientific, industrial and medical purposes. Unlike commercial nuclear power plants (NPPs), RRs are characterized by small core size, low total thermal power, high power density, low fuel and clad temperatures and low system pressure. Furthermore, the different fuel composition, geometric configuration and different ranges of relevant operational parameters constitute different neutronic and thermal-hydraulics designs [1-4].

As a result, these reactors must meet different safety requirements and unique safety features to ensure their safe utilization in nominal and off-nominal operation conditions and safe shutdown in case of an emergency or an accident. The reactor safety analysis report is frequently updated and must include the analysis of a wide variety of safety related scenarios. Furthermore, the uniqueness of each RR and its experimental systems makes the standardization of design, operation and licensing of RRs almost impractical, unlike commercial NPPs [2,5].

---

\* Corresponding author

The safety analysis methodology employed for existing NPPs is based on a well-established and very active international community of experts, well founded and proven methods and computational tools including best-estimate codes and uncertainty analysis, international standardization and extensive and accessible experimental database [1,6]. During the last decade, the IAEA and others [1,5,7] have acknowledged the importance of implementing the well-founded and mature NPP safety technology (methods, codes, regulations and guidelines) in RRs safety analysis methodology and reassess their safety features [4].

Recently, the adequacy of applying NPP computational tools to RRs has been addressed in several studies. For example, calculation of thermal-hydraulic transients in RRs using system codes such as RELAP5 [3-4,8-13], ATHLET [14], PARET [8,12,15], COBRA [16], RETRAC-PC [17-18], as well as coupled NK/TH calculations using PARCS/RELAP5 [19]. The majority of these studies consider the IAEA safety benchmark for 10 MW MTR light water pool-type reactor [20-21]. This benchmark was specified under the program of research reactor core conversions from highly enriched uranium (HEU) to low enriched uranium (LEU) cores. The benchmark consists of a detailed steady-state and transient neutron kinetics and thermal-hydraulic calculations for a wide range of accident scenarios.

The HEU core of this IAEA 10 MW MTR reactor is also considered in the present study. The three dimensional neutron flux and power distribution, as well as other kinetic parameters and burnup calculations, were performed using the latest version of the three-dimensional continuous-energy Monte Carlo reactor physics code Serpent [22]. A set of representative RIA and LOFA transients were calculated using coupled NK/TH code THERMO-T, which was developed for this purpose. The coupled calculation scheme and the physical and thermal-hydraulic models are validated by comparison of the results to the IAEA benchmark report [21], as well as to previous relevant studies, e.g. [7,19,23].

The main goal of this study is to evaluate the newly developed code's TH capabilities and to study the adequacy of using the Serpent code for obtaining the core neutronic parameters. This is a first stage in the development of a more advanced transient system code for MTR accidents modeling, which is already in progress, where the 3D deterministic neutronic nodal diffusion code DYN3D [24] would be integrated and utilized as the core neutron kinetics simulation tool.

## **2. DESCRIPTION OF COMPUTATIONAL TOOLS AND METHODS**

The main objective of the code, which is still under development, is to adequately calculate coupled NK/TH transients in a standard research reactor, such as RIA, LOFA, partial or full channel blockage and more. At this stage, the code utilizes point reactor model for describing the spatial and temporal dynamics of the neutron flux in the reactor core, using neutronic parameters and flux shape functions calculated by the Serpent code, i.e. full core 3D radial and axial neutron flux and power distributions. The thermal hydraulic model of the code consists of a primary coolant loop, including the core, the piping, a heat exchanger and a main circulation pump. The core can be represented using any number of channels by applying any desired mapping scheme between fuel channels and thermal hydraulic channels, using the appropriate radial power distribution. At this stage, the thermal hydraulic code solves one-dimensional single-phase steady state and transient flows, based on three conservation equations for the mass, momentum, and energy, a heat generation model and heat transfer equations for the fuel and clad.

## 2.1. The Neutronic Model

### 2.1.1. The point reactor model

The reactor power is derived by solving the point kinetic equations with six groups of delayed neutrons [25], where the axial and radial power distributions are calculated using Serpent,

$$\begin{aligned}\frac{dp(t)}{dt} &= \frac{\rho(t, T_C, T_F) - \beta_{\text{eff}}}{\Lambda} p(t) + \sum_{j=1}^6 \lambda_j c_j(t) \\ \frac{dc_j(t)}{dt} &= \frac{\beta_j}{\Lambda} p(t) - \lambda_j c_j(t)\end{aligned}\quad (1)$$

where  $p$  is the reactor power,  $\beta_{\text{eff}}$  is the delayed neutron fraction,  $\Lambda$  is the neutron generation time,  $\rho$  is the total reactivity,  $\beta_j$  is the relative delayed neutron fraction of group  $j$ ,  $c_j$  is the precursor concentration of group  $j$ , and  $\lambda_j$  is the decay constant of precursor group  $j$ .

The coupling of the neutron kinetics model to the thermal hydraulic conditions in the core is realized through the dependence of the reactivity on the fuel and coolant temperature, i.e.

$$\rho(t, T_C, T_F) \equiv \rho_{\text{ex}}(t) - \alpha_F \Delta T_F - \alpha_c \Delta T_c, \quad (2)$$

where  $\rho_{\text{ex}}(t)$  is an induced external reactivity,  $\alpha_F$  and  $\alpha_c$  are the reactivity feedback coefficients of the fuel and coolant temperatures, respectively, and  $\Delta T_F$  and  $\Delta T_c$  are the deviation of the temperatures from their steady state values, i.e.  $\Delta T_x = T_x - T_{x,ss}$ .

### 2.1.2. The Serpent code

Serpent is a three dimensional continuous energy Monte Carlo neutron transport code with burnup capabilities developed at VTT research center in Finland [22]. The code was developed as an alternative to deterministic lattice physics codes for the generation of homogenized multigroup constants for reactor analyses using nodal codes. The current version of Serpent supports different nuclear evaluated data libraries, where for this study the ENDF/B-VII library was used.

A full 3D core model was developed for the MTR reactor HEU core [20-21]. The core consists of  $6 \times 5$  grid, containing 21 standard fuel assemblies and 4 control assemblies. Each standard fuel assembly consists of 23 fuel plates whereas the control fuel assembly contains 17 fuel plates, as shown in Fig. 1. The core configuration for both for Beginning of Life (BOL) and End of Life (EOL) is shown in Fig. 2 as a function of  $^{235}\text{U}$  depletion. The core is reflected on two of its sides with graphite reflectors and surrounded by water. The active core height is 60 cm, followed by 15 cm of axial Al-H<sub>2</sub>O reflectors containing volume fractions of 20% and 80% of Al and water, respectively. The main core parameters are summarized in Table 1.

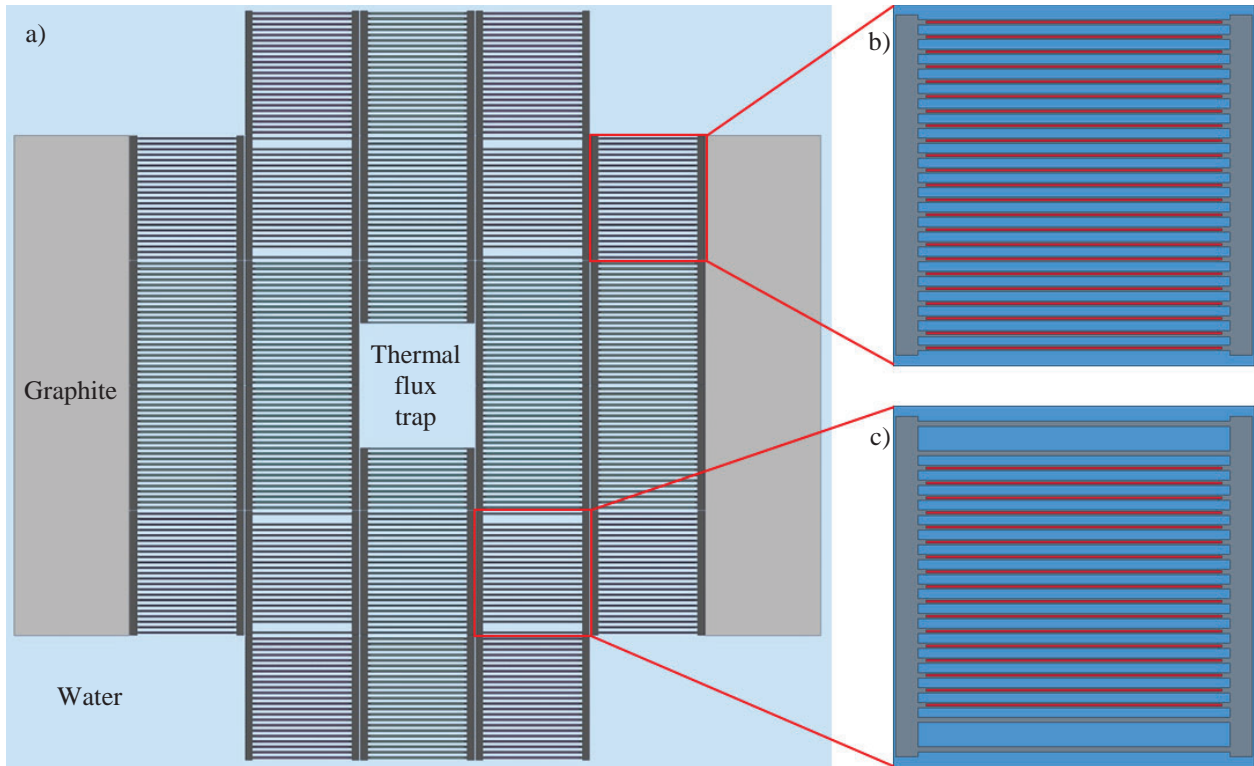


Figure 1. a) A two dimensional mid-plane cross section of the full MTR core as modeled using Serpent. b) standard fuel assembly. c) control fuel assembly.

Water	Water	Fuel BOL 5% EOL 10%	Fuel BOL 25% EOL 30%	Fuel BOL 5% EOL 10%	Water	Water
Graphite	Fuel BOL 5% EOL 10%	Control BOL 25% EOL 30%	Fuel BOL 45% EOL 50%	Control BOL 25% EOL 30%	Fuel BOL 5% EOL 10%	Graphite
Graphite	Fuel BOL 25% EOL 30%	Fuel BOL 45% EOL 50%	Fuel BOL 45% EOL 50%	Fuel BOL 45% EOL 50%	Fuel BOL 25% EOL 30%	Graphite
Graphite	Fuel BOL 25% EOL 30%	Fuel BOL 45% EOL 50%	Water	Fuel BOL 45% EOL 50%	Fuel BOL 25% EOL 30%	Graphite
Graphite	Fuel BOL 5% EOL 10%	Control BOL 25% EOL 30%	Fuel BOL 45% EOL 50%	Control BOL 25% EOL 30%	Fuel BOL 5% EOL 10%	Graphite
Water	Water	Fuel BOL 5% EOL 10%	Fuel BOL 25% EOL 30%	Fuel BOL 5% EOL 10%	Water	Water

Figure 2. IAEA MTR reactor HEU core configuration as a function of  $^{235}\text{U}$  depletion [20].

**Table I. IAEA MTR core parameters used for 3D power distribution calculation using Serpent [20].**

<b>Active core height</b>	600 mm
<b>Space at the grid plate per fuel assembly</b>	77×81 mm
<b>Fuel assembly</b>	76×80.5 mm (including support plate)
<b>Meat dimensions</b>	63×0.51×600 mm
<b>Density of aluminum-cladding</b>	2.7 g/cm <sup>3</sup>
<b>Support plate thickness / density</b>	4.75 mm / 2.7 g/cm <sup>3</sup>
<b>Fuel Plate Thickness</b>	1.27 mm
<b>UAl<sub>x</sub>-Al HEU fuel</b>	Enrichment 93 w/o U <sup>235</sup> 280 gU <sup>235</sup> per fuel element 21 w/o of uranium in the UAl <sub>x</sub> -Al
<b>Total power</b>	10 MWth
<b>Water temperature</b>	20 °C
<b>Fuel temperature</b>	20 °C

## 2.2. The Thermal Hydraulic Model

### 2.2.1. Coolant model

In order to calculate the thermal hydraulic conditions in the core, a thermal hydraulic response code was developed at Ben-Gurion University called THERMO-T. This code solves the three conservation equations (mass, momentum and energy) in time and space and allows for the core to be divided into any required number of channels, from one lumped thermal hydraulic node and up to the number of fuel elements (one-to-one mapping), including the possibility for calculating an average channel alongside a hot channel. Each channel is divided into a specified number of axial nodes (in this study each channel was divided into 60 axial nodes of height 1 cm each).

### 2.2.2. Fuel heat transfer model

The fuel plate consists of fuel meat surrounded by cladding with appropriate dimensions (see Table 1) and the coolant channel is defined as the coolant region between two parallel fuel plates. Given the dimensions of the fuel plate and the flow conditions, it is reasonable to assume that the heat diffusion rate inside the fuel plate is negligible compared to the time derivative of the fuel enthalpy and the power. Furthermore, in RIA transient the convection term on the water side is expected to be much larger than the heat diffusion term in the direction across the fuel plate. This assumption implies a uniform fuel plate temperature in the plane normal to the axial flow direction. In that case, the heat conduction term vanishes and the equations for the local fuel, clad and coolant temperatures,  $T_f(z,t)$ ,  $T_{cl}(z,t)$ , and  $T_c(z,t)$  become:

$$\begin{aligned}
 \rho_F V_F C_F \frac{\partial T_F(z,t)}{\partial t} &= p(z,t) - UA[T_F(z,t) - T_{cl}(z,t)] \\
 \rho_{cl} V_{cl} C_{cl} \frac{\partial T_{cl}(z,t)}{\partial t} &= UA[T_F(z,t) - T_{cl}(z,t)] - hA[T_{cl}(z,t) - T_c(z,t)] \quad , \\
 \rho_c A_c C_c \frac{\partial T_c(z,t)}{\partial t} &= hA[T_{cl}(z,t) - T_c(z,t)] - \dot{m}C_c \frac{\partial T_c(z,t)}{\partial z}
 \end{aligned}
 \tag{3}$$

where  $p(z,t)$  is the local fission power and  $U$  is the overall heat transfer coefficient between the fuel and the cladding. The coupling of the thermal hydraulic model to the neutron kinetics model is realized through the fission power term  $p(z,t)$  appearing in the equation for the fuel temperature.

### 2.3. The Numerical Scheme

The point kinetics equation are solved at each time step using a semi-implicit scheme of the form

$$\begin{aligned} \frac{p^{n+1} - p^n}{\Delta t} &= \frac{\rho^n - \beta_{\text{eff}}}{\Lambda} p^n + \sum_{j=1}^6 \lambda_j c_j^{n+1} \\ \frac{c_j^{n+1} - c_j^n}{\Delta t} &= \frac{\beta_j}{\Lambda} p^n - \lambda_j c_j^{n+1} \end{aligned} \quad , \quad (4)$$

where  $n$  denotes the variable's value at time  $t_n = n\Delta t$ . This discretization leads to the following iterative procedure at each time step (excluding relaxation factors for clarity)

$$\begin{aligned} c_j^{k+1} &= \left( c_j^k + \Delta t \frac{\beta_j}{\Lambda} p^k \right) \times \left( 1 + \Delta t \lambda_j \right)^{-1} \\ p^{k+1} &= p^k + \Delta t \left( \frac{\rho^n - \beta_{\text{eff}}}{\Lambda} p^k + \sum_{j=1}^6 \lambda_j c_j^{k+1} \right) \end{aligned} \quad , \quad (5)$$

where  $k$  is the iteration index. The process is terminated once the convergence criterion  $|p^{k+1} - p^k|/p^k \leq \varepsilon$  is satisfied. The three conservation equations for the mass, momentum and energy of the coolant are solved in time and space by utilizing explicit temporal and spatial discretization assuming constant system pressure. The equation for the fuel heat transfer model is discretized explicitly:

$$\begin{aligned} \rho_F V_F C_F \frac{T_F^{n+1} - T_F^n}{\Delta t} &= p^n - UA(T_F^n - T_{cl}^n) \\ \rho_{cl} V_{cl} C_{cl} \frac{T_{cl}^{n+1} - T_{cl}^n}{\Delta t} &= UA(T_F^n - T_{cl}^n) - hA(T_{cl}^n - T_c^n) \\ \rho_c V_c C_c \frac{T_c^{n+1} - T_c^n}{\Delta t} &= hA(T_{cl}^n - T_c^n) - \dot{m} C_c \left( \frac{T_{c,out}^n - T_{c,in}^n}{\Delta z} \right) \end{aligned} \quad . \quad (6)$$

The values of the numerical parameters, e.g. time step size, number of axial nodes, iterative relaxation parameters, were optimized after careful considerations and repeated trials until the desired accuracy and stability were achieved.

## 3. RESULTS AND DISCUSSION

### 3.1. Power Distribution Calculation using Serpent

In order to improve the accuracy of the thermal hydraulic calculations we obtained the radial and axial power distributions from a full core 3D static calculation using Serpent. The calculated relative radial power distribution of the HEU core is shown in Fig. 3, whereas the calculated core average axial power distribution is shown in Fig. 4.

water	water	4.04±0.01 4.10±0.01	3.47±0.01 3.50±0.01	4.05±0.01 4.10±0.01	water	water
graphite	4.28±0.02 4.31±0.01	3.74±0.01 3.72±0.01	3.75±0.01 3.68±0.01	3.74±0.01 3.72±0.01	4.25±0.01 4.32±0.02	graphite
graphite	3.96±0.01 3.98±0.01	4.43±0.00 4.36±0.02	2.67±0.01 2.60±0.02	4.45±0.02 4.36±0.02	3.97±0.00 3.98±0.01	graphite
graphite	3.96±0.01 3.98±0.01	4.43±0.00 4.36±0.01	Water 2.67±0.01 2.61±0.01	4.43±0.00 4.35±0.02	3.97±0.00 3.97±0.02	graphite
graphite	4.25±0.01 4.31±0.01	3.74±0.01 3.72±0.02	3.76±0.01 3.69±0.01	3.74±0.01 3.72±0.02	4.25±0.01 4.31±0.01	graphite
water	water	4.04±0.01 4.11±0.01	3.49±0.01 3.50±0.01	4.05±0.01 4.10±0.01	water	water

Figure 3. The calculated relative radial power distribution of the HEU core using Serpent. Upper and lower values denote the power distribution at BOL and EOL, respectively.

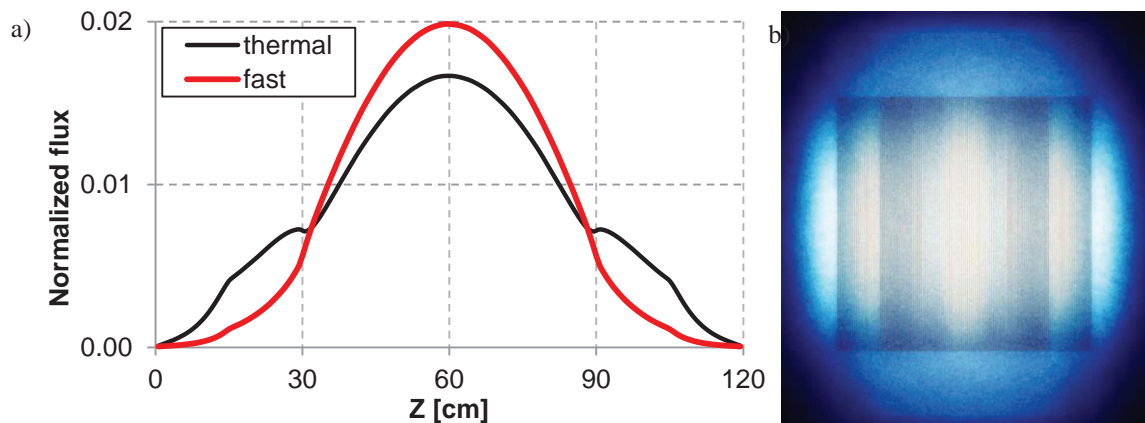


Figure 4. a) The calculated relative axial flux distribution of the HEU core using Serpent. The active fuel region spans between  $z=30-90$  cm. b) A cross section in the middle  $x-z$  plane of the HEU core depicting the thermal flux and fission rate distribution.

### 3.2. Protected RIA Transient

The protected Fast RIA transient in the HEU core, as defined in the IAEA benchmark, is initiated by a super prompt ramp positive reactivity insertion at a rate of  $\$1.5/0.5$  s. The initial conditions are an operating power of 1 W at BOL and fully developed steady state coolant flow. The safety system SCRAM trip point is set at 120% of the reactor's nominal operating power, i.e. at 12 MW, and it inserts negative reactivity at a rate of  $10\$/0.5$  s with a response delay time of 0.025 s. A comprehensive list of the benchmark parameters can be found in [20].

In order to examine the core thermal hydraulic partitioning and choice of channels, the HEU Fast RIA transient was calculated using three different thermal hydraulic models: a) a single channel model, where the core is considered as a single lumped channel, b) 2-channels model, where the core is represented by an average channel and a hot channel, and c) full core one-to-one mapping of thermal hydraulic channels to fuel elements. In each case, the reactivity feedbacks were properly averaged between the different channels and the radial and axial power distributions were taken from the Serpent calculation. The core power evolution during Fast RIA for HEU core is shown in Fig. 5 for the three different thermal hydraulic models. The RIA transient is initiated at time  $t=0.5$  s.

Initially, the power increases exponentially, reaching a maximum just before the SCRAM system trips. Once the control rods are inserted, the prompt response of the core power, followed by the delayed neutrons response at about  $t=0.7$  s after transient initiation, is evident in Fig. 5. It is clear that all three models produce very similar results throughout the entire transient, except for relatively small differences in peak power value. In fact, the SCRAM system trips at the same time for all three models (around  $t=0.606$  after transient initiation). Moreover, the results presented in Fig. 5 show that the lumped channel model and full core model exhibit a slightly higher peak power level in the hot channel during the transient. The 2-channels model and the full core channel show good agreement with respect to RELAP5 and PARET results [19], better than the lumped channel model.

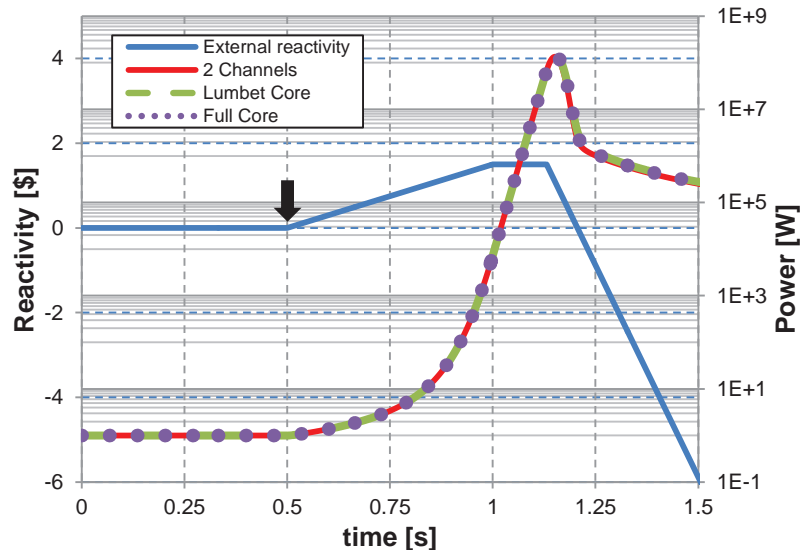


**Figure 5. Peak power during HEU Fast RIA using three different thermal hydraulic models. The black arrow marks the starting point of the transient ( $t=0.5$  s).**

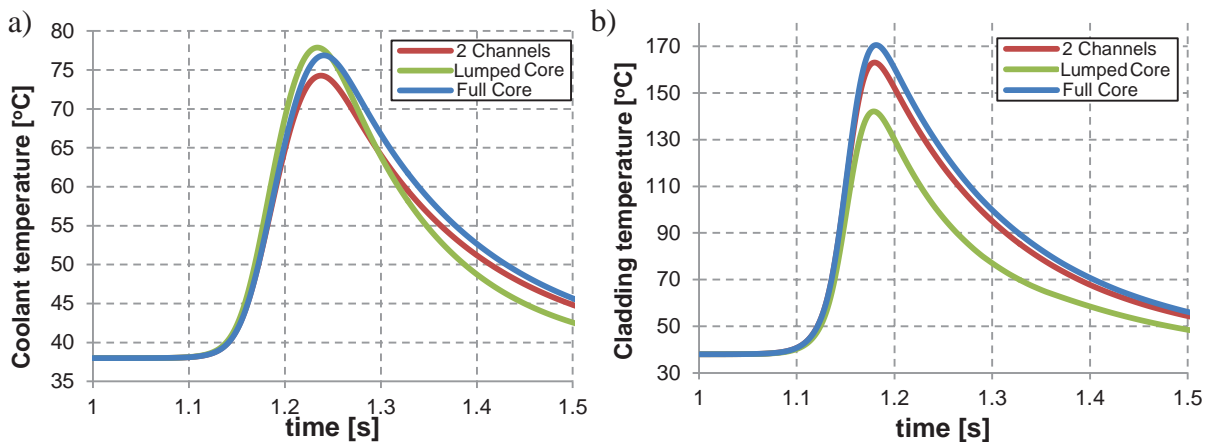


**Figure 6. Coolant outlet (a) and cladding (b) peak temperatures during HEU Fast RIA.**

The clad and coolant temperature starts increasing during the control rods insertion, at approximately the same time as the core power reaches its maximum value, as shown in Fig. 6. The peak clad and coolant temperatures lag behind the core's peak power by approximately 0.03 and 0.08 s, respectively. The transient main results are summarized in Table II.

**Table II. Fast RIA in HEU core results<sup>1</sup>.**

TH model	Lumped	2-channels	full core	RELAP5*	PARET*
trip [s]	0.613	0.606	0.606	0.609	0.609
Peak power [MW]	142.5 (0.652)	134 (0.652)	141 (0.653)	131 (0.655)	129 (0.655)
Peak clad temp. [°C]	142.1 (0.679)	163.0 (0.68)	170.2 (0.684)	163.3 (0.673)	155.3 (0.672)
Peak coolant temp. [°C]	77.87 (0.734)	74.23 (0.737)	76.9 (0.741)	78.90 (0.770)	84.3 (0.760)

\*from [19].

### 3.3. Sensitivity to Heat Transfer Correlation Type

In order to evaluate the code's sensitivity to the heat transfer correlation type, four different correlations for forced convective turbulent flow [26] were implemented and tested against the HEU Fast RIA transient benchmark: Sleicher-Rouse [27] (Eq. 7), Seider-Tate [28] (Eq. 8), Dittus-Boelter [29] (Eq. 9), and Petukhov [30] (Eq. 10). It was found that the correlation which exhibits the best agreement with the results presented in the benchmark is that of Sleicher-Rouse [27]. The corresponding peak power values and peak outlet temperatures are shown in Fig. 7 and summarized in Table III. All four curves were calculated using the 2-channels model of average and hot channels. The pronounced differences in both peak power and outlet temperature makes the choice of heat transfer correlation crucial for adequate accuracy of the results when compared to experimental results.

$$\begin{aligned}
 Nu &= 5 + 0.015 Re^a Pr^b \\
 a &= 0.88 - 0.24 / (4 + Pr) \\
 b &= 0.333 + 0.5e^{-0.6Pr}
 \end{aligned} \tag{7}$$

$$Nu = 0.027 Re^{4/5} Pr^{1/3} (\mu/\mu_s)^{0.14} \tag{8}$$

$$Nu = 0.027 Re^{4/5} Pr^{2/5} \tag{9}$$

$$\begin{aligned}
 Nu &= \frac{(f/8) Re Pr}{K_1 + K_2 (f/8)^{0.5} (Pr^{2/3} - 1)} \cdot (\mu/\mu_s)^{0.14} \\
 f &= (1.58 \ln(Re) - 3.28)^{-1} \\
 K_1 &= 1 + 3.4f \\
 K_2 &= 11.7 + 1.8 Pr^{-1/3}
 \end{aligned} \tag{10}$$

**Table III. Fast RIA in HEU core results for different heat transfer correlations<sup>1</sup>.**

Correlation	Sleicher-Rouse [27]	Seider-Tate [28]	Dittus-Boelter [29]	Petukhov [30]
Peak power [MW]	134 (0.652)	124.8 (0.651)	126.3 (0.651)	155.5 (0.655)
Peak cladding temp. [°C]	163.0 (0.68)	141.8 (0.675)	145.7 (0.676)	219.6 (0.696)
Peak coolant temp. [°C]	74.23 (0.737)	77.21 (0.731)	76.57 (0.732)	58.20 (0.759)

<sup>1</sup> The number in parenthesis is the time after transient initiation at which the peak value occurred.

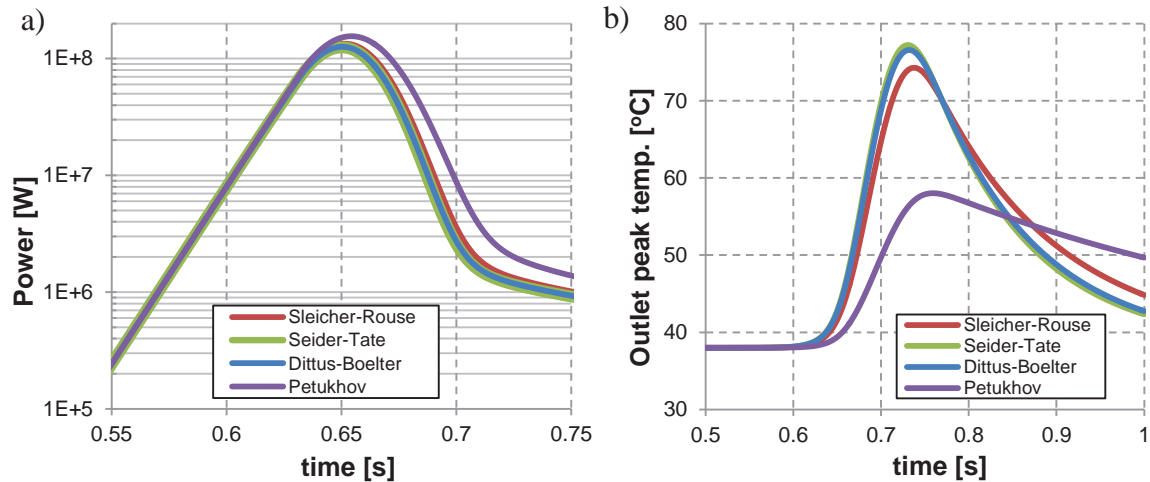


Figure 7. Power (a) and coolant outlet (b) peak values during HEU Fast RIA using different heat transfer correlation.

### 3.4. Protected LOFA Transient

The protected Fast LOFA transient, as defined in the IAEA benchmark, is initiated by a main coolant pump coast down while the reactor operates at nominal conditions. The flow decay is modeled according to  $exp(-t/\tau)$  where  $\tau=1$  s for fast LOFA. This transient is characterized by the fuel heat up and strong thermal hydraulic interaction between the fuel and the coolant loop via the reactivity feedbacks. The LOFA transient is initiated at a nominal core power of 12 MW and fully developed coolant flow conditions. The reactor SCRAM system trips when the flow decay reaches 85% of the nominal flow rate, with a response delay time of 0.2 s.

The evolution of the core power, and clad and coolant outlet temperatures during the first 2 seconds of a protected Fast LOFA transient in HEU core, as well as the corresponding mass flow rate and reactivity feedbacks are plotted in Fig. 8. At the beginning of the transient, the fuel and coolant temperatures increases due to the coolant flow rate decay, resulting in a mild and steady core power decrease. Once the scram system trips, the control rods are inserted into the core, accompanied by a sharp decrease in the fuel and coolant temperatures. Eventually, the core temperature decreases enough such that the heat generated in the fuel is fully removed by the coolant natural flow. The Fast LOFA transient was calculated using the 2-channels model, with a representative average channel and a hot channel. The main results from the Fast LOFA transient are summarized in Table III and compared to previously published results.

Table III. Fast LOFA in HEU core results<sup>1</sup>.

TH mode	THERMO-T	RELAP5*	PARET*
Core power at scram [MW]	11.6 (0.163)	11.9 (0.200)	11.9 (0.295)
1 <sup>st</sup> peak cladding temperature [°C]	90.8 (0.385)	91.3 (0.408)	87.5 (0.376)
1 <sup>st</sup> peak coolant temperature [°C]	53.9 (0.427)	59.5 (0.503)	60.9 (0.602)
Cladding temperature at 15% of nominal flow [°C]	44.7	49.3	48.2
Coolant temperature at 15% of nominal flow [°C]	41.2	46.8	47.2

\* from [7].

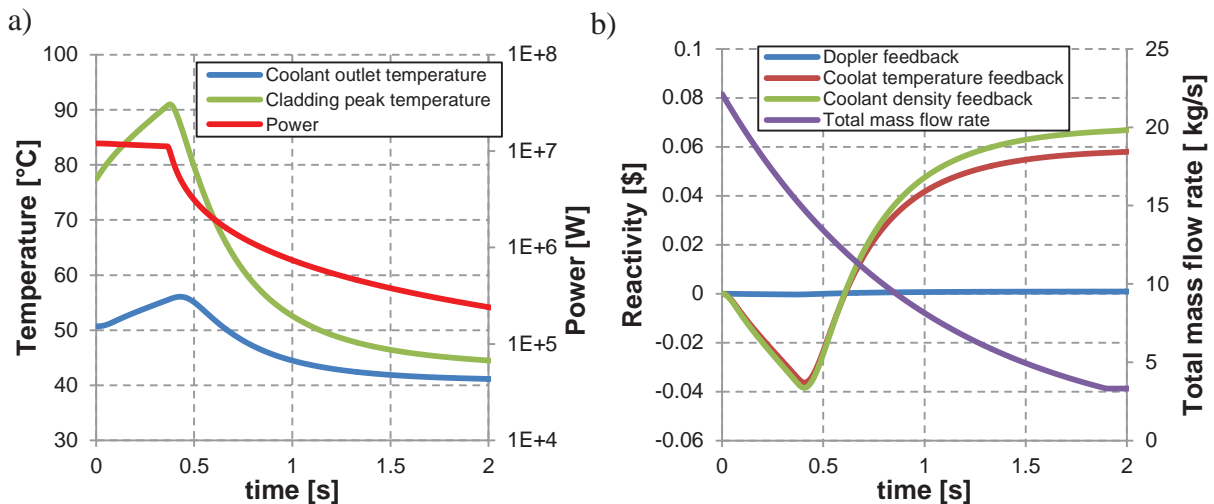


**Figure 8. The first 2 seconds of a protected Fast LOFA transient in HEU core. a) core power, clad and coolant outlet temperatures, and b) mass flow rate and reactivity feedbacks.**

#### 4. CONCLUSIONS

A coupled NK/TH code (THERMO-T) was developed and applied to the analysis of protected reactivity insertion (RIA) and loss of flow (LOFA) accidents in a typical research reactor with standard MTR plate type fuel assemblies. While the code is under development, in this paper we report the first stages of its validation by comparing its results to those of other codes, such as RELAP5 and PARET. The code exhibits good capabilities in predicting the thermal hydraulic conditions in the core during both Fast RIA and Fast LOFA transients.

We have demonstrated that all three thermal hydraulic models, i.e. single lumped channel, 2-channels (average and hot), and full core, produce very similar results throughout the entire transients, except for relatively small differences in peak power value. Moreover, the results presented in Fig. 5 (Table II) show that the lumped channel model and full core model exhibit a slightly higher peak power level in the hot channel during the transient. Overall, the 2-channels model and the full core channel show good agreement with respect to RELAP5 and PARET results [19].

The code's sensitivity to the choice of heat transfer correlation was evaluated. It was found that different heat transfer correlations lead to pronounced differences in both peak power and coolant outlet temperature. This fact makes the choice of heat transfer correlation crucial for adequate accuracy of the results when compared to experimental results. It was found that the correlation which exhibits the best agreement with the results presented in the benchmark is that of Sleicher-Rouse [27].

Finally, we have shown that the Serpent code is capable of producing a correct radial and axial power distributions in the core, and in the future more advanced capabilities of the Serpent code will be put to the test, such as kinetic parameters calculations and the generation of homogenized multigroup cross section for the 3D deterministic neutronic nodal diffusion code DYN3D, that is currently being integrated into THERMO-T as a 3D core neutron kinetics solver.

#### ACKNOWLEDGMENTS

The authors would like to express their deepest appreciation and gratitude to Dr. Alex Rashkovan from NRCN for his contribution for this study.

## REFERENCES

1. F. D'Auria and A. Bousbia-Salah, "Accident analysis in research reactors," Proceedings of the 15<sup>th</sup> Pacific basin nuclear conference, Sydney, Australia, Oct 15-20 2006, pp. 88-93 (2006).
2. T. Hamidouche, A. Bousbia-Salah, E.K. Si-Ahmed and F. D'Auria, "Overview of accident analysis in nuclear research reactors," *Prog. Nucl. Energy* **50**(1), pp. 7-14 (2008).
3. M. Adorni, A. Bousbia-salah, F. D'Auria and T. Hamidouche, "Application of Best Estimate thermalhydraulic codes for the safety analysis of research reactors," Proceedings of the International Conference on Nuclear Energy for New Europe 2006, Portoroz, Slovenia, Sep 18-21 2006, pp. 621.1-621.10 (2006).
4. M. Adorni, A. Bousbia-salah, F. D'Auria and T. Hamidouche, "Accident analysis in research reactors," Proceedings of the International Conference on Nuclear Energy for New Europe 2007, Portoroz, Slovenia, Sep 10-13 2007, pp. 202.1-202.9 (2007).
5. A.L. Costa, P.A.L. Reis, C.A.M. Silva, C. Pereira, M.A.F. Veloso, B.T. Guerra, H.V. Soares and A.Z. Mesquita, Safety Studies and General Simulations of Research Reactors Using Nuclear Codes, Nuclear Power - System Simulations and Operation, Dr. Pavel Tsvetkov (Ed.), InTech, Shanghai, China (2011).
6. A. Bousbia-Salah and F. D'Auria, "Use of coupled code technique for Best Estimate safety analysis of nuclear power plants," *Prog. Nucl. Energy* **49**(1), pp. 1-13 (2007).
7. T. Hamidouche, A. Bousbia-Salah, M. Adorni and F. D'Auria, "Dynamic calculations of the IAEA safety MTR research reactor Benchmark problem using RELAP5/3.2 code," *Ann. Nucl. Energy* **31**(12), pp. 1385-1402 (2004).
8. J.R. Deen, N.A. Hanan, R.S. Smith, J.E. Matos, P.M. Egorenkov and V.A. Nasonov, "Neutronic safety parameters and transient analyses for potential LEU conversion of the IR-8 research reactor," *Proceedings of the international meeting on Reduced Enrichment for Research and Test Reactors (RERTR)*, Budapest, Hungary, Oct 3-8 1999, (1999).
9. M. Adorni, A. Bousbia-Salah, T. Hamidouche, B. Di Maro, F. Pierro and F. D'Auria, "Analysis of partial and total flow blockage of a single fuel assembly of an MTR research reactor core," *Ann. Nucl. Energy* **32**(15), pp. 1679-1692 (2005).
10. M. Azzoune, L. Mammou, M.H. Boulheouchat, T. Zidi, M.Y. Mokeddem, S. Belaid, A. Bousbia-Salah, B. Meftah and A. Boumedien, "NUR research reactor safety analysis study for long time natural convection (NC) operation mode," *Nucl. Eng. Des.* **240**(4), pp. 823-831 (2010).
11. M.M. Bretscher, N.A. Hanan and J.E. Matos, "Neutronic safety parameters and transient analyses for Poland's MARIA research reactor," *Proceedings of the international meeting on Reduced Enrichment for Research and Test Reactors (RERTR)*, Budapest, Hungary, Oct 3-8 1999, (1999).
12. S. Chatzidakis, A. Hainoun, A. Doval, F. Alhabet, F. Francioni, A. Ikonomopoulos and D. Ridikas, "A comparative assessment of independent thermal-hydraulic models for research reactors: The RSG-GAS case," *Nucl. Eng. Des.* **268**, pp. 77-86 (2014).
13. A. Hedayat, H. Davilu and J. Jafari, "Loss of coolant accident analyses on Tehran research reactor by RELAP5/MOD3.2 code," *Prog. Nucl. Energy* **49**(7), pp. 511-528 (2007).
14. A. Hainoun and A. Schaffrath, "Simulation of subcooled flow instability for high flux research reactors using the extended code ATHLET," *Nucl. Eng. Des.* **207**(2), pp. 163-180 (2001).
15. C. Housiadas, "Simulation of loss-of-flow transients in research reactors," *Ann. Nucl. Energy* **27**(18), pp. 1683-1693 (2000).
16. S. Safaei Arshi, H. Khalafi and S.M. Mirvakili, "Preliminary thermal-hydraulic safety analysis of Tehran research reactor during fuel irradiation experiment," *Prog. Nucl. Energy* **79**, pp. 32-39 (2015).
17. A. Bousbia-Salah and T. Hamidouche, "Analysis of the IAEA research reactor benchmark problem by the RETRAC-PC code," *Nucl. Eng. Des.* **235**(6), pp. 661-674 (2005).
18. A. Bousbia-Salah, B. Meftah, T. Hamidouche and E.K. Si-Ahmed, "A model for the analysis of loss of decay heat removal during loss of coolant accident in MTR pool type research reactors," *Ann. Nucl. Energy* **33**(5), pp. 405-414 (2006).

19. T. Hamidouche, A. Bousbia-Salah, E.K. Si-Ahmed, M.Y. Mokeddem and F.D'Auria, "Application of coupled code technique to a safety analysis of a standard MTR research reactor," *Nucl. Eng. Des.* **239**(10), pp. 2104-2118 (2009).
20. IAEA, "Research Reactor Core Conversion from the Use of High-Enriched Uranium to the Use of Low Enriched Uranium Fuels Guidebook," IAEA-TECDOC-233 (1980).
21. IAEA, "Research reactor core conversion guidebook," IAEA-TECDOC-643 (1992).
22. J. Leppänen, "Development of a new Monte Carlo reactor physics code," D.Sc. Thesis, Helsinki University of Technology, (2007).
23. M.A. Gaheen, S. Elaraby, M.N. Aly and M.S. Nagy, "Simulation and analysis of IAEA benchmark transients," *Prog. Nucl. Energy* **49**(3), pp. 217-229 (2007).
24. U. Grundmann, U. Rohde, and S. Mittag, "DYN3D – Three-dimensional core model for steady-state and transient analysis of thermal reactors," *Proceedings of the 2000 ANS International Topical Meeting on Advances in Reactor Physics and Mathematics and Computations into the Next Millennium (PHYSOR 2000)*, Pittsburgh, USA, May 7-11 2000, (2000).
25. G.R. Keepin, *Physics of nuclear kinetics*, Addison-Wesley, Reading, Mass. (1965).
26. C.P. Tzanos, "Predictions of the heat transfer coefficient by correlations and turbulence models," *Nucl. Technol.* **183**(1), pp. 88-100 (2013).
27. C.A. Sleicher and M.W. Rouse, "A convenient correlation for heat transfer to constant and variable property fluids in turbulent pipe flow", *Int. J. Heat Mass Transfer* **18**, pp 677-683(1975).
28. E.N. Sieder and G.E. Tate, "Heat transfer and pressure drop of liquids in tubes", *Ind. Eng. Chem.*, **28**(12), pp. 1439-1435(1936).
29. F.W. Dittus and L.M.K. Boelter, "Heat transfer in automobile radiators of the tubular type", *Int. Comm. Heat Mass Transfer*, **12**, pp.3-22(1985).
30. B.W. Petukhov, "Heat transfer and function in turbulent pipe flow with variable physical properties" in J.P. Harlett and T.F. Irvine (eds), *Advances in Heat Transfer*, Academic Press, New York (1970).